

Supporting Information for

Intraoperative Detection and Eradication of Residual Microtumors with Gap-Enhanced Raman Tags

Yuanyuan Qiu,^{†,‡,◆} Yuqing Zhang,^{§,‡,◆} Mingwang Li,^{†,‡,◆} Gaoxian Chen,^{†,‡} Chenchen Fan,^{†,‡} Kai Cui,^{†,‡} Jian-Bo Wan,[▽] Anpan Han,[○] Jian Ye,^{,§,⊥} Zeyu Xiao^{*,†,‡,||,♯}*

[†]Department of Pharmacology and Chemical Biology, and [‡]Translational Medicine Collaborative Innovation Center, Institute of Medical Sciences, School of Medicine, [§]State Key Laboratory of Oncogenes and Related Genes, School of Biomedical Engineering, ^{||}Institute of Molecular Medicine, and [⊥]Shanghai Key Laboratory of Gynecologic Oncology, Ren Ji Hospital, School of Medicine, [♯]Collaborative Innovation Center of Systems Biomedicine, Shanghai Jiao Tong University, Shanghai, P. R. China

[▽]State Key Laboratory of Quality Research in Chinese Medicine, Institute of Chinese Medical Sciences, University of Macau, Taipa, Macao, China

[○]DTU Danchip/CEN, Technical University of Denmark, Kgs. Lyngby, Denmark

[‡]College of Life Information Science and Instrument Engineering, Hangzhou Dianzi University, Hangzhou, P.R. China

*Email address for corresponding author: zxiao@sjtu.edu.cn (Z.X.) or yejian78@sjtu.edu.cn (J.Y.)

◆ Y.Q. and Y.Z. and M. L. contributed equally to this work.

Methods

Chemicals. Chloroauric chloride ($\text{HAuCl}_4 \cdot 4\text{H}_2\text{O}$), ascorbic acid, tetraethyl orthosilicate (TEOS), sodium hydroxide (NaOH) and methanol were purchased from Sinopharm Chemical Reagent Co. Ltd (Shanghai, China). Sodium borohydride (NaBH_4 , 98%), cetyltrimethylammonium chloride (CTAC, 98%) and D-Luciferin potassium salt were obtained from J&K Chemical Ltd (Shanghai, China). 1, 4-Benzenedithiol (BDT, 98%) was received from TCI (Tokyo, Japan). Cell Counting Kit-8 (CCK-8) was purchased from Thermo Fisher Scientific (USA). Cell Viability Assay Kit for differentiating live or dead cells was obtained from Sangon Biotech (Shanghai, China).

Stability Measurements of GERTs. The physiological stability of GERTs was evaluated by incubating GERTs with 100% fetal bovine serum (FBS) at 37 °C, and SERS spectra were collected at 0, 4, 12, 24, 48, 72, and 96 h. To evaluate the Raman signal stability of GERTs, GERTs (0.2 nM) in 100% FBS was continuously irradiation for 60 min with a power density of $4.7 \times 10^5 \text{ W/cm}^2$. SERS spectra were acquired at 2 min interval (785 nm laser, 1.86 s exposure time, and 5× objective). The laser power density was calculated as follows:

$$\text{laser power density} = \frac{\text{laser power}}{\text{laser spot area}}$$

Where laser power is 37 mW, and the laser spot diameter is 3.2 μm in the photostability test.

Evaluation of the Photothermal Depths of GERTs. We used a tissue-mimicking phantom to investigate the photothermal efficiency of GERTs with increasing penetration depths. The tissue-mimicking phantom was made of agarose solution consisting of 2% agarose to mimic tissue absorption and 0.5% liposyn to mimic tissue scattering.

GERTs (0.25 nM) were dispersed in 50 μL of agarose solution and then left to solidify in a plastic cylindrical container with a diameter of 6.8 mm. Subsequently, additional blank agarose solution was poured onto the GERTs-mixed agarose layer to create a serial of depths ranging from 0 to 9.63 mm. The tissue-mimicking phantom was then irradiated by an 808 nm laser at the power of 3.6 W/cm^2 for 5 min, with adjusted laser spot to cover the entire bottom of the cylindrical container. The temperature was recorded by an infrared (IR) thermal imaging camera (DT-980, CEM Co. Ltd, Shenzhen, China) every 30 s.

Calculating the Photothermal Transduction Efficiency. GERTs dispersions (100 μL) were continuously irradiated by an 808nm laser at a power of 1.05 W until reaching a steady state temperature. The laser was then turned off and the temperature decrease was monitored to measure the rate of heat transfer (Figure 4C). According to Roper's report, the photothermal conversion efficiency (η) was calculated using eqn (1).

$$\eta = \frac{hA(T_{\max} - T_{\text{amb}}) - Q_0}{I(1 - 10^{-A_\lambda})} \quad (1)$$

where h is the heat transfer coefficient, A is the surface area of the container, T_{\max} is the maximum system temperature, T_{amb} is the ambient surrounding temperature, and $(T_{\max} - T_{\text{sur}})$ is 23.8°C according to Figure 4C. I is the laser power (1.05 W) and A_λ is the absorbance (0.1217) at an excitation wavelength of 808 nm. Q_0 represents heat dissipated from light absorbed by the solvent. The value of Q_0 can be measured directly as eqn (2).

$$Q_0 = hA(T_{\max, \text{solvent}} - T_{\text{amb}}) \quad (2)$$

The Q_0 was measured independently using the same container containing pure water without the GERTs. $T_{\max, \text{solvent}}$ is the maximum solvent temperature, and $(T_{\max, \text{solvent}} - T_{\text{amb}})$ is 0.1°C . The lumped quantity hA was determined by measuring the rate of temperature drop after removing the light source. The value of hA is derived according to eqn (3):

$$hA = \frac{m_D C_D}{\tau_S} \quad (3)$$

where m_D is the mass (0.0991 g), C_D is heat capacity (4.2 J/ g) of deionized water used as solvent, and τ_S is the time constant. To measure τ_S , a dimensionless term θ is introduced:

$$\theta = \frac{T - T_{amb}}{T_{max} - T_{amb}} \quad (4)$$

θ is determined by Figure 4C, where T_{amb} is the ambient surrounding temperature, T_{max} is the maximum system temperature, and T is the temperature at different time point. By calculating linear time data from the cooling period of Figure 4C (Y axe in Figure 4D) *versus* negative natural logarithm of driving force temperature ($-\ln\theta$, X axe in Figure 4D), the slope of Figure 4D is determined to be τ_S (113.5 s). Thus, the 808 nm laser heat conversion efficiency (η) of the GERTs can be calculated to be 33.8%.

Calcein AM/PI Staining. PC-3M-luc-C6 cells were cultured in glass bottom 24-well plate with a density of 2×10^4 cells until grown to 80 ~ 90% confluency. Next, cells were replaced with Ham's F-12K medium containing GERTs and incubated for 5 h. After washing with PBS for three times, the cells were immersed in 200 μ L of fresh culture medium, followed by irradiation with the laser beam (808 nm, 3.6 W/cm²) for 5 min. Cells treated with GERTs or laser irradiation barely were set as control. After removing F-12K medium, Cell Viability Assay Kit was applied to differentiate live or dead cells of all groups. Fluorescence images of cells were obtained by confocal microscopy (TCS SP8, Leica).

Transmission Electron Microscopy (TEM) Images of Tumor Tissues. Tumor tissues were fixed in a solution of 2.5% glutaraldehyde. Samples were then stained with 1% osmium tetroxide in water at 4 °C for 2 h. Later on, the tissue samples were rinsed with deionized water and stained with 1% uranyl acetate at 4°C overnight. Samples

were then dehydrated in progressively higher concentrations of ethanol at 4°C, 50%, 70%, and 95%. The tissue samples were then allowed to gradually warm to room time. Samples were further dehydrated in 100% ethanol and in propylene oxide. Samples were then embedded in Embed 812 epoxy resin. Samples were placed in 1:1 solution of Embed 812: propylene oxide for 1 h at room time, and then placed in 2:1 solution of Embed 812: propylene oxide overnight. Finally samples were placed in 100% Embed 812 for 1 h before being placed in molds and cured overnight at 60 °C. Thin sections (120 nm) were then cut from the tissue samples using an ultramicrotome (Leica EM UC7, Leica, Germany) and placed on copper grids. The sections were examined without coverslip using a TEM operating at 80 kV (Tecnai G2 Spirit Biotwin, FEI, USA).

Statistical Analysis. Experiment results were presented as mean \pm SD. Statistical significance was calculated on the basis of the Student's t-test (two-tailed, unpaired), and $P < 0.05$ was considered statistically significant.

Supporting Figures

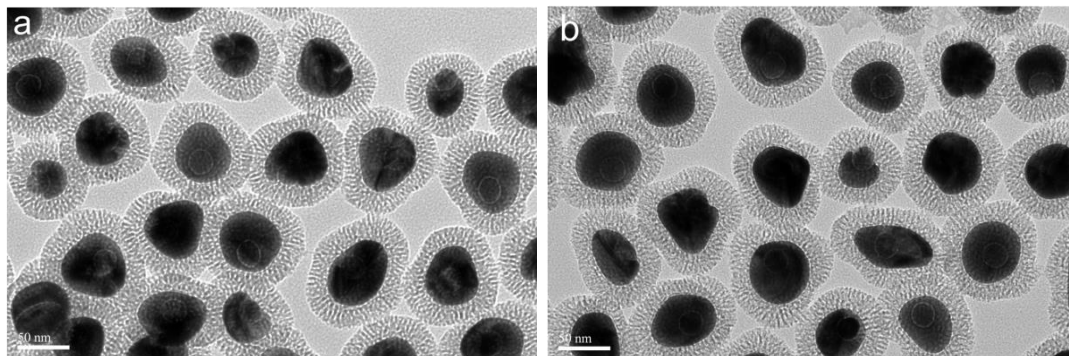


Figure S1. TEM images of a large number of GERTs demonstrate their uniform size distribution. The scale bar is 50 nm.

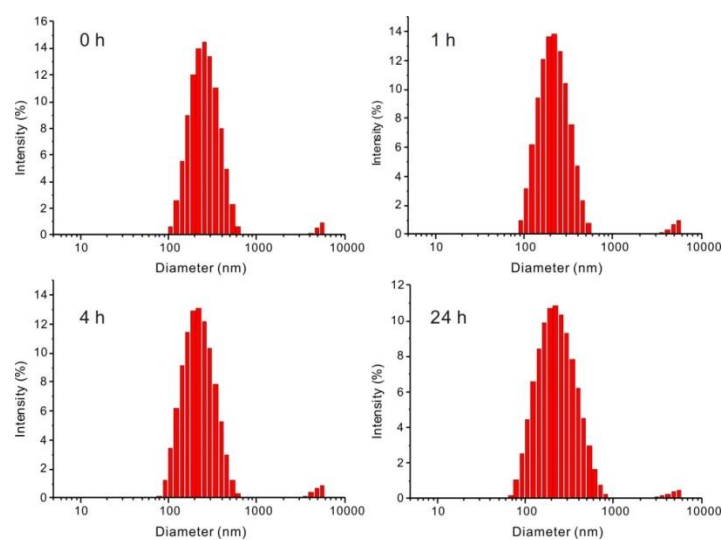


Figure S2. The hydrodynamic size of GERTs during the incubation in cell culture media with 10% FBS for 24 h, measured by dynamic light scattering (DLS).

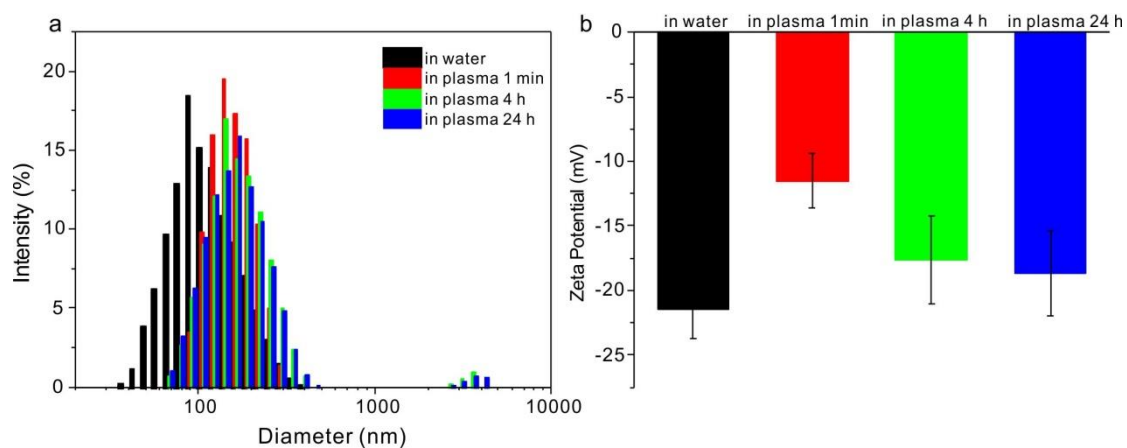


Figure S3. The hydrodynamic sizes (a) and zeta potentials (b) of GERTs in water and in plasma at 1 min, 4 h, and 24 h, respectively.

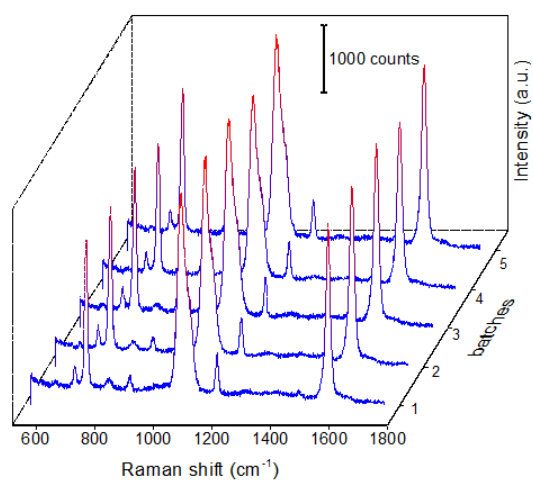


Figure S4. Raman spectra of aqueous GERTs (0.2 nM, 20 mW, 1.0 s acquisition time, 10 \times objective) in 5 different batches indicate their highly uniform Raman signals.

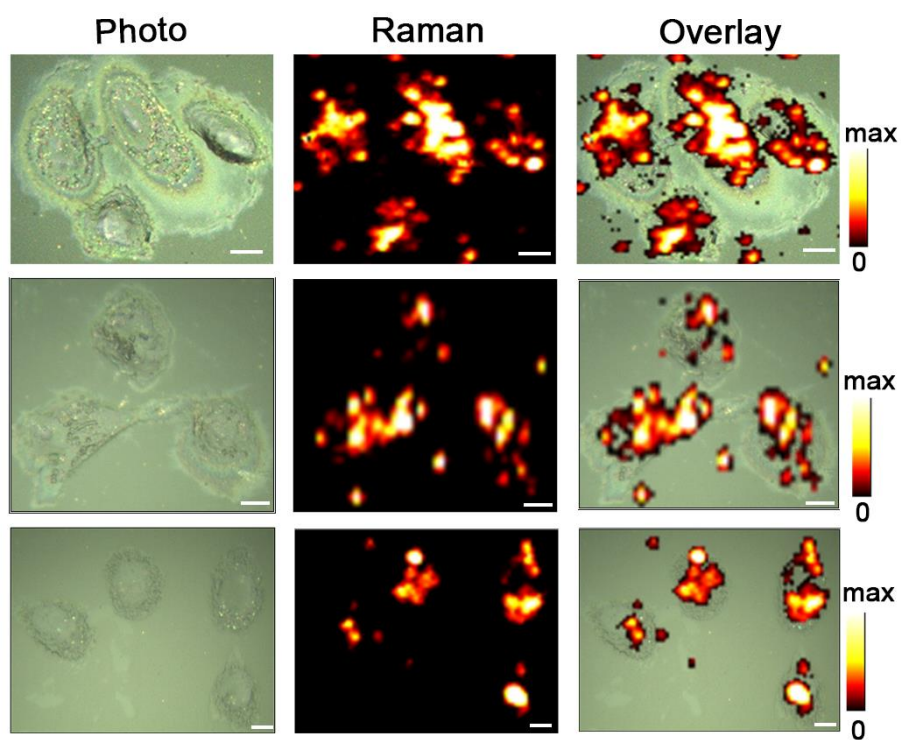


Figure S5. Raman images of multiple cells pre-incubated with GERTs. All scale bars are 10 μm . Colors are assigned to the signals of Raman characteristic band of GERTs at 1555 cm^{-1} .

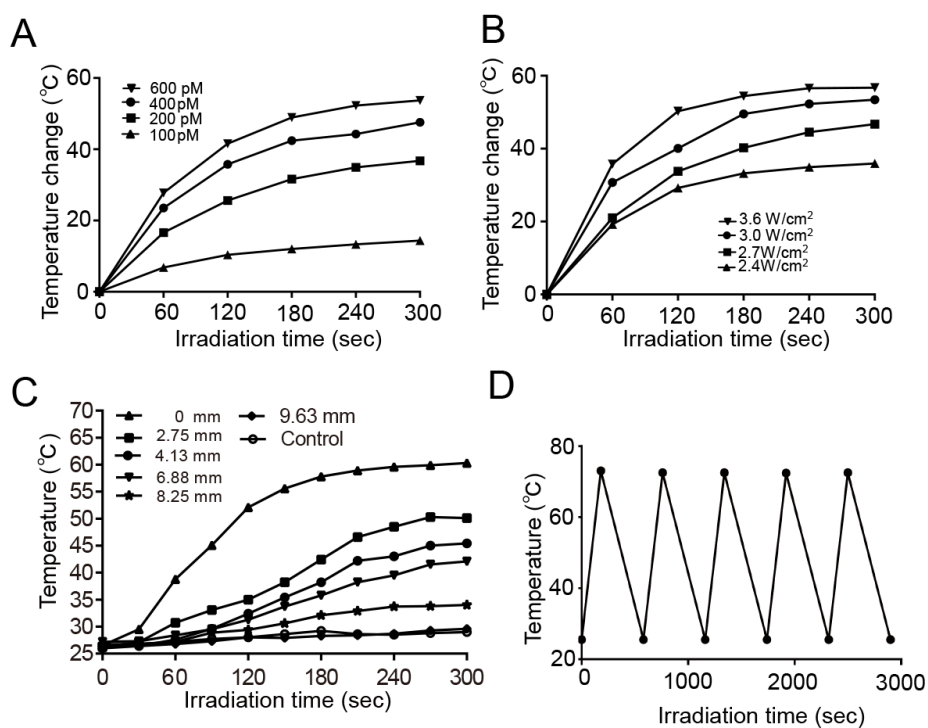


Figure S6. *In vitro* photothermal ablation test. Photothermal heating profiles of GERTs (A) with different concentrations or (B) under different intensities of 808 nm laser irradiation. (C) Temperature curves of tissue-mimicking phantom containing GERTs at increasing depths. (D) Temperature changes of GERTs under five laser ON/OFF cycles at 3.6 W/cm².

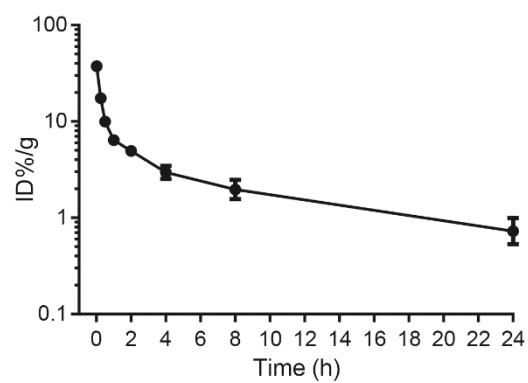


Figure S7. Blood circulation of GERTs within 24 h, calculated by the Au percentage relative to injected dose (ID) per gram of the blood.

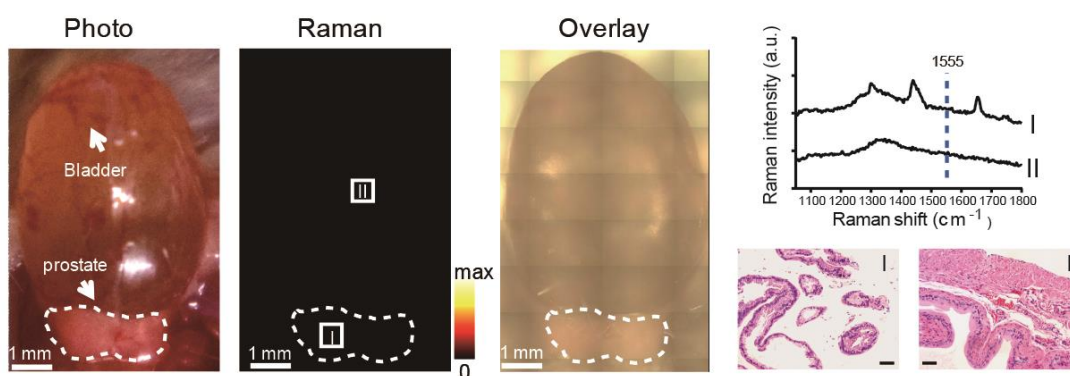


Figure S8. *In vivo* Raman image of normal prostate and bladder at 20 h post-intravenous injection of GERTs. White dotted line indicates prostate. None of the characteristic Raman signals of GERTs at 1555 cm^{-1} (the blue dash line) were detected in prostate and bladder. Hematoxylin and eosin (H&E) staining confirmed the tissue sections from normal prostate (I) and bladder (II) (scale bars are 50 μm).

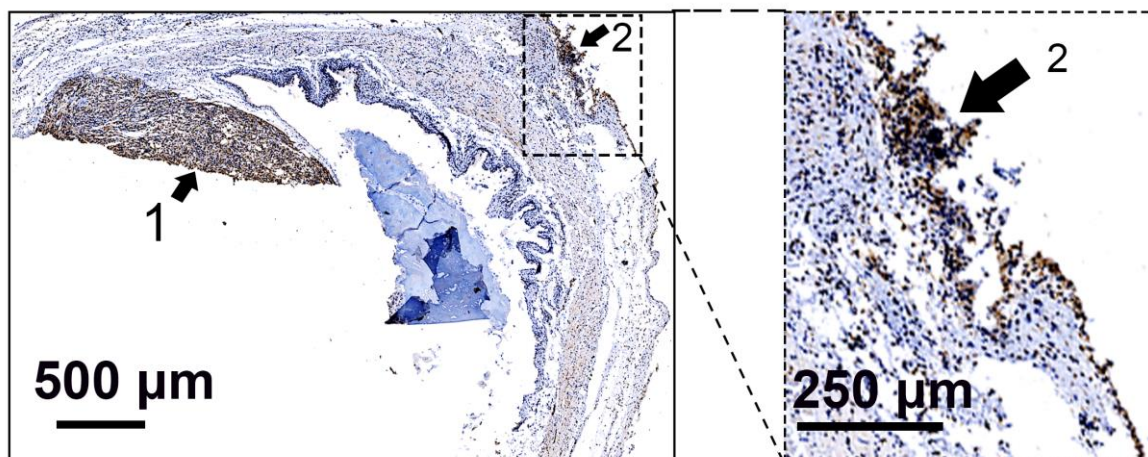


Figure S9. Immunohistochemical staining for NSE. Arrow 1 and arrow 2 indicated residual tumors around resection bed and metastasized to the bladder, respectively.

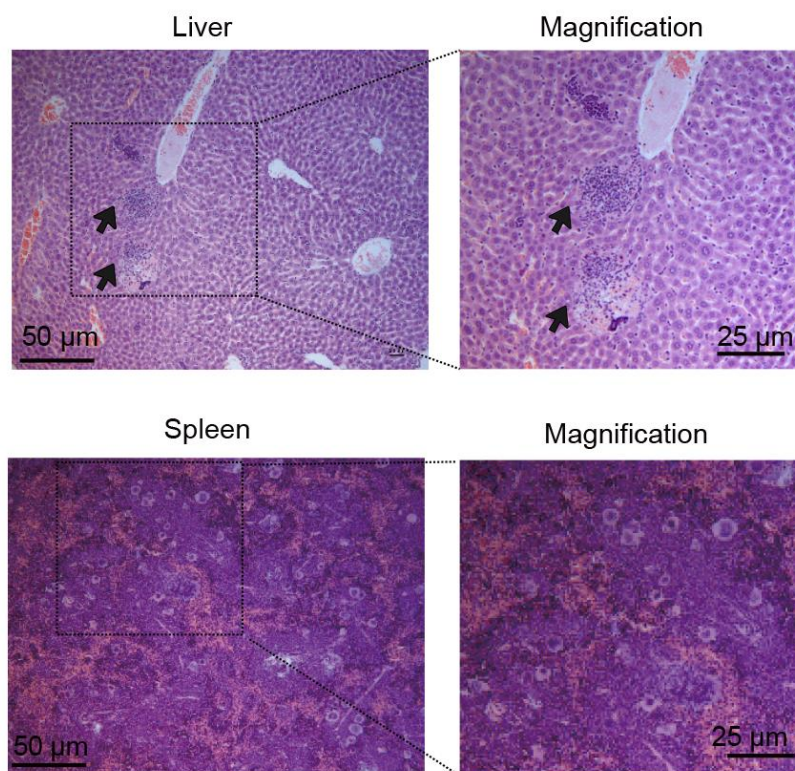


Figure S10. H&E staining of the liver and spleen of tumor bearing-mice in PBS group. Metastatic lesions (black arrows) exist in the liver. Dramatic inflammation exists in the spleen.